sensors

MDPI

Article

Flexible Piezoelectric Energy Harvesting from Mouse Click Motions

Youngsu Cha [1,*], Jin Hong [1,2], Jaemin Lee [1], Jung-Min Park [1] and Keehoon Kim [1]

[1] Center for Robotics Research, Korea Institute of Science and Technology, Seoul 02792, Korea; hoji0207@kist.re.kr (J.H.); jmlee87@kist.re.kr (J.L.); pjm@kist.re.kr (J.-M.P.); khk@kist.re.kr (K.K.)

[2] School of Mechanical Engineering, Korea University, Seoul 02841, Korea

* Correspondence: givemong@kist.re.kr; Tel.: +82-2-958-6949

Academic Editor: Dan Zhang

Received: 8 June 2016; Accepted: 4 July 2016; Published: 6 July 2016

Abstract: In this paper, we study energy harvesting from the mouse click motions of a robot finger and a human index finger using a piezoelectric material. The feasibility of energy harvesting from mouse click motions is experimentally and theoretically assessed. The fingers wear a glove with a pocket for including the piezoelectric material. We model the energy harvesting system through the inverse kinematic framework of parallel joints in a finger and the electromechanical coupling equations of the piezoelectric material. The model is validated through energy harvesting experiments in the robot and human fingers with the systematically varying load resistance. We find that energy harvesting is maximized at the matched load resistance to the impedance of the piezoelectric material, and the harvested energy level is tens of nJ.

Keywords: energy harvesting; mouse click motion; piezoelectric material

1. Introduction

Recent advancements and developments in the area of wearable devices have stimulated the demand for energy harvesting system [1–3]. Various energy sources, such as heat [4] and motions [5–7], in human body can be converted into useful electric energy by using energy transducers. In this context, energy harvesting to support the power of wearable devices using the human body energy sources can offer several benefits: permanent lifetime and weight reduction through the needlessness of batteries [8].

Piezoelectric materials are a good solution as energy transducer [9,10]. Especially, Lead zirconate titanate (PZT) [11–13], Polyvinylidene fluoride (PVDF) [14–17], Macro-fiber composite (MFC) [18–21], Aluminum nitride (AlN) [22], and Zinc oxide (ZnO) [23] have been used as typical energy transducers. They convert the kinetic energy of surrounding environment into electric energy. For example, energy harvesting from PVDF when subjected to various wind speeds and water droplets has been evaluated in [14]. The feasibility of energy generation of PVDF cantilever with a magnetic mass has been experimentally studied in [15]. PVDF is the most flexible piezoelectric material among them although it has the lowest electromechanical coupling [24,25]. The flexibility can offer important advantage in the development of wearable devices by reducing the inconvenience of wearing.

Here, we theoretically and experimentally study energy harvesting using the flexible energy transducer, PVDF, attached to robot and human index fingers during mouse click motions. The ability of harvesting energy from mouse click motions may be applicable to the development of self-powered computer mouse [26], wearable mouse glove [27], or hand motion recognition device [28]. Various researches about energy harvesting using human motions have been reported. For instance, energy harvesting from foot strike during human walking by using shoes including PZT and PVDF has been introduced in [5]. In [29], human walking motion has been also used for

energy harvesting by using a backpack instrumented with piezoelectric shoulder straps. In [30], a device using plucked piezoelectric bimorphs for energy harvesting from knee motions during human walking has been reported. Energy harvesting on human limb motions has been demonstrated in [6]. In [7], energy harvesting using the jaw movements of human through the piezoelectric chin strap has been demonstrated. Energy harvesting from two different piezoelectric transducers attached to the human body for five human activities has been studied in [31]. Interestingly, a glove to harvest electric energy from the kinetic energy of the fingers has been reported in [32]. Therein, four couples of piezoelectric transducers have been integrated into the glove in correspondence with the fingers joints, but the finger motions for energy harvesting have not been specified. Moreover, ZnO based energy harvester using stretched and released states of index finger has been demonstrated in [33]. In this work, we focus on the mouse click motions of fingers for energy harvesting. Specifically, we model the mouse click motions and the energy transducing of the piezoelectric material. The proposed model is validated through experiments using robot and human index fingers. The energy transducer, PVDF, is attached to fingers by wearing a glove with a pocket for piezoelectric material. In the robot finger, we can reduce the effect by the variation of the human motion, and quantitatively analyze the energy harvesting from the mouse click motions. From a practical point of view, this work addresses the untapped research question of energy harvesting from mouse click motions. From a methodological point of view, the main contributions of this effort are: (i) developing an electromechanical model to study energy harvesting of flexible piezoelectric materials bent by mouse click motions; (ii) performing a thorough experimental campaign to validate the proposed modeling framework in various conditions, whereby one and double click motions, human and robot fingers, and shunting load resistance; and (iii) conducting a systematic analysis of its energy harvesting capacity.

This paper is organized as follows. In Section 2, we introduce the proposed modeling framework, including the inverse kinematic framework of parallel joints in a finger and the electromechanical coupling for the energy transducer. In Section 3, we describe the experimental scheme developed to study energy harvesting from the mouse click motions. In Section 4, we report and discuss the experimental results toward the validation of the model and the analysis of harvested energy from the mouse click motions of a robot finger and a human index finger. Conclusions are summarized in Section 5.

2. Modeling

2.1. Finger Model

The formulation of the model for index finger motion follows the inverse kinematic framework of parallel joints presented in [34] for studying human hand movements. Therein, the finger can be considered locally a three degree of freedom mechanism with three links in a plane, see Figure 1. The origin of the coordinate system lies at the index metacarpophalangeal (MP) joint. The angle of rotation of the MP joint is defined as ϕ_{MPJ}. The angles of the other two joints are labeled as ϕ_{PIJ} (proximal interphalangeal (PI) joint) and ϕ_{DIJ} (distal interphalangeal (DI) joint) [35]. The lengths of the three links are L_1 (proximal phalanx), L_2 (middle phalanx), and L_3 (distal phalanx) [35]. Moreover, we denote r and α with the distance between the tip and the origin of the finger and the angle between r and the starting position of the MP joint ($\phi_{\mathrm{MPJ}} = 0$), respectively.

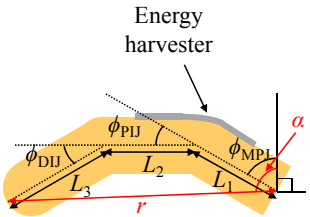

Figure 1. Schematic of parallel joints on finger.

Following [34], the relationship among the lengths and distance is given by

$$\begin{aligned}
&(L_1^2 + L_2^2 + L_3^2 - r^2 - 2L_1L_2 - 2L_1L_3 + 2L_2L_3)g^{10} \\
&+ (5L_1^2 + 5L_2^2 + 5L_3^2 - 5r^2 + 26L_1L_2 + 90L_1L_3 - 6L_2L_3)g^8 \\
&+ (10L_1^2 + 10L_2^2 + 10L_3^2 - 10r^2 + 28L_1L_2 - 420L_1L_3 - 28L_2L_3)g^6 \\
&+ (10L_1^2 + 10L_2^2 + 10L_3^2 - 10r^2 - 28L_1L_2 + 420L_1L_3 - 28L_2L_3)g^4 \\
&+ (5L_1^2 + 5L_2^2 + 5L_3^2 - 5r^2 - 26L_1L_2 - 90L_1L_3 - 6L_2L_3)g^2 \\
&+ (L_1^2 + L_2^2 + L_3^2 - r^2 + 2L_1L_2 + 2L_1L_3 + 2L_2L_3) = 0
\end{aligned} \tag{1}$$

where g is an unknown variable related with the rotation angles. When we know L_1, L_2, L_3, and r, Equation (1) can be solved with at least two real solutions for g. Herein, we use the built-in function 'Solve' in MATHEMATICA (www.wolfram.com) to solve it. Among the solutions, the only valid solution in a reachable position is the positive real one. From the solution g, we obtain [34]

$$\phi_{\mathrm{MPJ}} = \alpha - \arccos\left(\frac{s^2 - r^2 - L_1^2}{2rL_1}\right) \tag{2}$$

$$\phi_{\mathrm{PIJ}} = 6\arctan(g) \tag{3}$$

$$\phi_{\mathrm{DIJ}} = 4\arctan(g) \tag{4}$$

where $s = \sqrt{L_2^2 + L_3^2 - 2L_2L_3\cos(\pi - \phi_{\mathrm{DIJ}})}$.

We comment that the variations of the angles can be obtained through Equations (1)–(4) and the distance r changed by mouse click motions, without directly measuring the angles. In particular, we note that ϕ_{PIJ} and ϕ_{DIJ} are related to only the solution g.

2.2. Energy Harvesting Model

An energy harvester using a piezoelectric material is attached to the PI joint. When we assume the energy harvester has a beam structure, its electrical response is described by a relationship between the charge stored in the structure and the rotation of the beam as [11,20,36]

$$Q(t) = CV(t) + \theta\tan(\phi_{\mathrm{PIJ}}(t)) \tag{5}$$

where Q is the stored charge, C is the internal capacitance of the piezoelectric material, V is the voltage between the both electrodes of the piezoelectric material, θ is the electromechanical coupling coefficient, and t is the time variable.

When the piezoelectric material is open-circuited ($Q = 0$), the voltage is reduced as

$$V_{\mathrm{oc}}(t) = -\frac{\theta\tan(\phi_{\mathrm{PIJ}}(t))}{C} \tag{6}$$

Moreover, when a load resistor R_{load} is shunted to the piezoelectric material, the load voltage V_{load} is given by Ohm's law, that is,

$$\frac{\mathrm{d}Q(t)}{\mathrm{d}t} = -\frac{V_{\mathrm{load}}(t)}{R_{\mathrm{load}}} \tag{7}$$

By combining Equations (5) and (7), we derive

$$C\frac{\mathrm{d}V_{\mathrm{load}}(t)}{\mathrm{d}t} + \theta\frac{\mathrm{d}\tan(\phi_{\mathrm{PIJ}}(t))}{\mathrm{d}t} = -\frac{V_{\mathrm{load}}(t)}{R_{\mathrm{load}}} \tag{8}$$

By numerically solving Equation (8) with the given $\phi_{\mathrm{PIJ}}(t)$ using MATHEMATICA by the built-in function 'NDSolve', we obtain the load voltage.

Additionally, we can calculate the energy transferred to the load resistor E_{load} from the piezoelectric material during $t = T$, following

$$E_{\mathrm{load}} = \int_0^T \frac{V_{\mathrm{load}}^2(t)}{R_{\mathrm{load}}} \mathrm{d}t \tag{9}$$

The integral is numerically computed using hundreds of Gaussian quadrature points at the selected cases to reduce the computational time.

3. Experiments

3.1. Experimental Setup

The energy harvester has the unimorph beam structure to consist of PVDF as a piezoelectric material and mylar as a substrate, see a similar example in [16]. Specifically, a PVDF produced by Measurement Specialties (www.meas-spec.com) is glued on a thin mylar using epoxy 3 M DP460. The dimensions of the PVDF and mylar layers are $28 \times 8 \times 0.028\,\mathrm{mm}^3$ and $25 \times 8 \times 0.1\,\mathrm{mm}^3$, respectively. The PVDF surface is slightly bigger due to the connection with electrodes. Conductive adhesive 3 M copper foil tape 1181 is used for the both side electrodes. The overall structure is sealed with 3 M Scotch tape. Figure 2a displays the top view of the energy harvester used in this study.

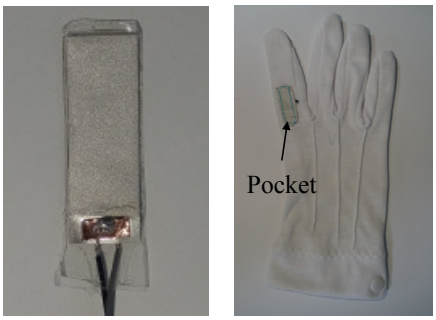

Figure 2. Pictures of (**a**) the piezoelectric composite and (**b**) the glove with the pocket.

To attach the energy harvester to a finger, we use a reform glove with a pocket, see Figure 2b. The experimental setup using a human finger is displayed in Figure 3. The human index finger has the size of $L_1 = 41\,\mathrm{mm}$, $L_2 = 22\,\mathrm{mm}$, and $L_3 = 20\,\mathrm{mm}$. All experiments are conducted on Logitech M-U0026 mouse. SONY FDR-AX30 camera is utilized to acquire the finger movements, and Xcitex Proanalyst software (www.xcitex.com) is used to track the selected markers on the finger. The resolution of the camera is set to 1920×1080 pixels, and the recording rate is 60 frame/s. The recoding camera image scale is approximately 0.01 cm/pixel in the experiments.

The output voltage from the piezoelectric material is acquired using National Instrument data acquisition (DAQ) board 6343 and a custom-made code in Labview (www.ni.com/labview). The input impedance of the DAQ board is $10\,\mathrm{G}\Omega$ in parallel with 100 pF, and the sampling rate is 2000 Hz. During experiments, the piezoelectric material is open-circuited or shunted with a load resistance varied from 1 to $99\,\mathrm{M}\Omega$ by using IET LABS RS-201W resistance decade box. A MATLAB (www.mathworks.com) script is utilized to remove the power source noise from the output voltage through a 2-order low pass Butterworth filter at 30 Hz. The capacitance of the piezoelectric material, $C = 1.58\,\mathrm{nF}$, is measured using FLUKE-17B+ digital multimeter.

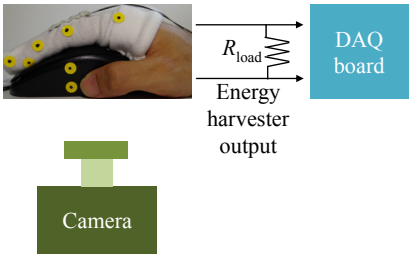

Figure 3. Experimental setup for a human finger.

3.2. Robot Finger

In the second phase of the experimental study, we use a robot finger [37,38] for studying the energy harvesting. The prosthetic robot finger is designed to generate finger motions such as pinch grasping motion, see Figure 4. Basically, the prosthetic finger system contains underactuated mechanism, which is a linkage mechanism, in order to implement compliant motion similar to human finger motion with respect to unknown grasping objects. The benefit of the underactuated mechanism is the reduction of the number of actuator in the robot system. Specifically, only one joint is actuated by a motor, and the other two joints are passively rotated by transferred power with the linkage mechanism. Therefore, the robot finger is able to generate human-like compliant motion. FAULHABER 1717T024SR DC-micro motor, controlled by MAXON LSC 30/2 servo amplifier and PC104 main controller, is used to actuate the robot finger and to receive the encoder signal with 1000 Hz. The main controller is programmable using MATLAB simulink. During the experiments, the robot finger wears also the glove including the energy harvester. Other experimental setup is same to Section 3.1. The experimental setup is displayed in Figure 5.

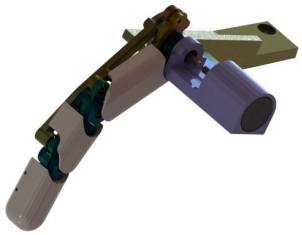

Figure 4. CAD model of a robot finger.

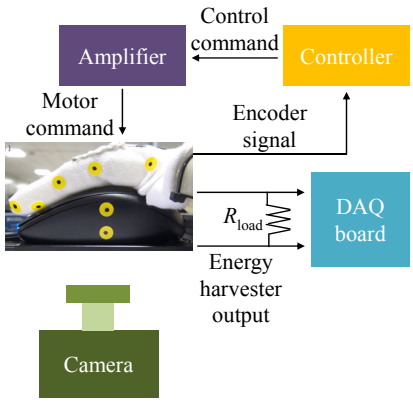

Figure 5. Experimental setup for a robot finger.

4. Results

4.1. Motion Trajectory of Human Finger

We capture the motion trajectory of the human index finger during a mouse one click and a double click. Specifically, the angles of the MP joint ϕ_{MPJ} are obtained by using the recoding camera data, see Figure 6. The human index finger during the mouse clicks has the tiny movements under 1° and approximately the frequency of 2–3 Hz. Additionally, to formulate the angle trajectory, we perform Fourier cosine series fitting by using the built-in function 'fit' in MATLAB. Figure 6 displays the fitting results including the fundamental harmonic of the angle. The coefficients of determination R-squared of the fitting are 0.9221 at the one click and 0.9029 at the double click. Therefore, the mouse click motions of the human index finger can be presented by a cosine function.

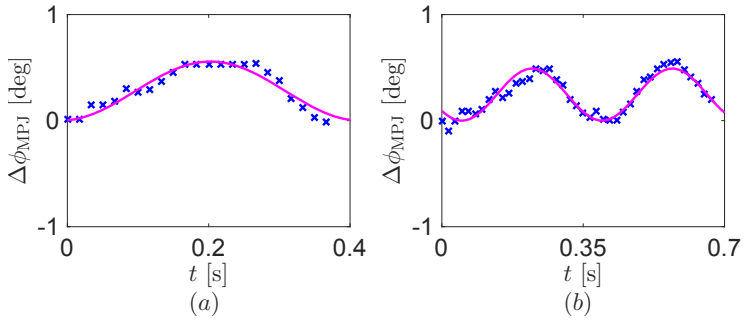

Figure 6. The angle ϕ_{MPJ} of the human index finger. (**a**) One click and (**b**) double click. Blue crosses and purple lines are the experimental data and its fundamental harmonics, respectively.

4.2. Operation of Robot Finger

The fitting results of the motion trajectory in Figure 6 are used for the operation of the motor in the robot finger. In the robot finger, we use the amplitude increased by 50% due to the friction at the connection between the motor and the robot finger. The angle ϕ_{MPJ} programmed in the robot finger is $a(1-\cos(2\pi f t))$ where $a = 0.4179^\circ$ and $f = 2.353$ at the one click, and $a = 0.3683^\circ$ and $f = 2.877$ at the double click. For the double click, we use two periods of the cosine function. Figure 7 displays the encoder signal from the robot finger. We comment that the angle from the encoder signal can be different with the real angle because of the friction at the connection in the robot finger.

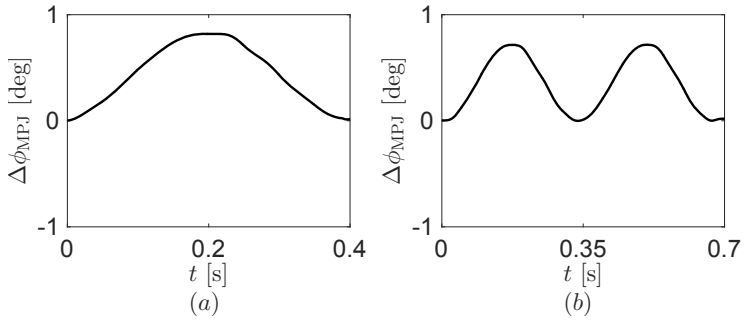

Figure 7. Encoder signal from the robot finger. (**a**) One click and (**b**) double click.

Figure 8 shows the distance r between the tip and the MP joint of the robot finger using the recoding camera data. To use the distance in the model of Section 2, we also fit the distance to the Fourier cosine series about the fundamental harmonic through MATLAB.

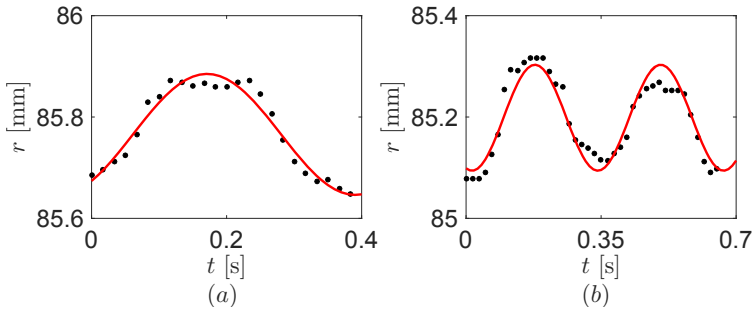

Figure 8. The distance r between the tip and the metacarpophalangeal (MP) joint of the robot finger. (**a**) One click and (**b**) double click. Black dots and red lines are the experimental data and its fundamental harmonics, respectively.

4.3. Open-Circuit Voltage from Robot Finger

To obtain the coupling coefficient θ of the energy harvester, we perform an experiment about its electrical responses at the open-circuited electrodes, that is, $R_{load} = \infty$ in Figure 5. In practice, the electrodes of the the energy harvester are shunted with the large input impedance of the DAQ board to record the voltage output. Such impedance is over one thousand times larger than the matching impedance of the piezoelectric material in the frequency of the mouse click motions, based on the measured capacitance. Figure 9 displays the open-circuit voltage output from the energy harvester during the both mouse click motions. The electrical responses are dominated by the fundamental harmonic at the frequency of the mouse click motions. We obtain $\theta = -158\,\mathrm{nJ/V}$ using the one click data of Figures 8 and 9 with the model in Section 2.

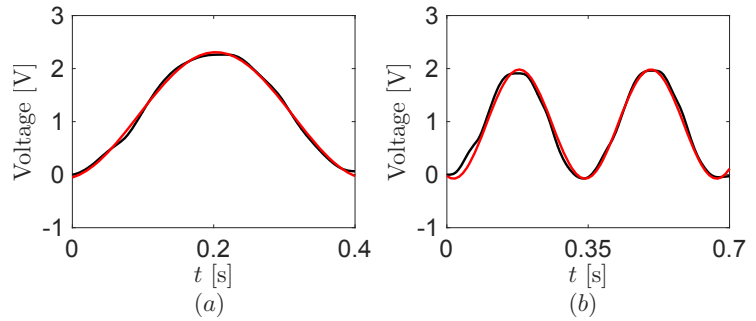

Figure 9. Open-circuit voltage output from the energy harvester. (**a**) One click and (**b**) double click. Black and red lines are the experimental data and its fundamental harmonics, respectively.

4.4. Energy Harvested from Robot Finger

The overall modeling framework in Section 2 allows for predicting the energy harvested at the load resistance R_{load}. Figure 10 illustrates the computation results of the harvested energy as a function of the load resistance. Therein, the harvested energy from the experiments is also overlapped. The comparison between the theoretical predictions and experimental results demonstrates that the model is fairly accurate in predicting the harvested energy varying the load resistance. The maximum harvested energy is in the range of 1–10 nJ at the both mouse clicks. Experimental results indicate that the harvested energy is maximized for load resistances on the range of 30–70 MΩ, which correspond to the matching impedance $1/(2\pi fC)$ of the piezoelectric material. Some discrepancy between the theoretical predictions and experimental results is likely to be attributed to the change of the electromechanical property by the movement and the initial curve of the energy harvester in the pocket during the experiments. Additionally, half harmonic frequency may be relevant in the double click experiments. It makes the maximum point move into higher one $(1/(\pi fC))$.

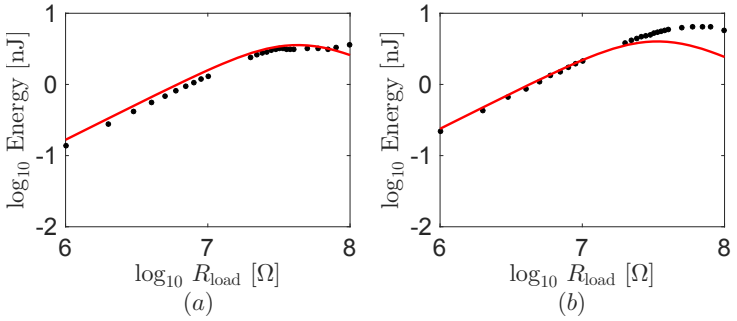

Figure 10. Theoretical predictions and experimental results on energy transferred to the load resistance as a function of the resistance using the robot finger. (**a**) One click and (**b**) double click. Black dots and red lines are the experimental results and the theoretical predictions, respectively.

4.5. Energy Harvested from Human Finger

We adapt the overall modeling framework for the harvested energy to the human finger. To reduce the effect of the variation of the human motion, we use the average value of the five repeated experiments at the each load resistance. Figure 11 displays the theoretical predictions and experimental results of the energy harvested from the human finger during the both mouse clicks. Although the human motions are not perfectly same for all trials unlike the robot, the theoretical predictions are also in good agreement with the experimental results in anticipating the trend of the energy as a function of the load resistance. The maximum energy harvested from the human finger is on the order of 1 nJ at the both mouse clicks. We note that the lower energy level of the human finger than the robot results from the structural difference by different size (L_1, L_2, and L_3)of the fingers. In other words, the different finger size of the human finger makes smaller $\Delta\phi_{\mathrm{PIJ}}$ than the robot.

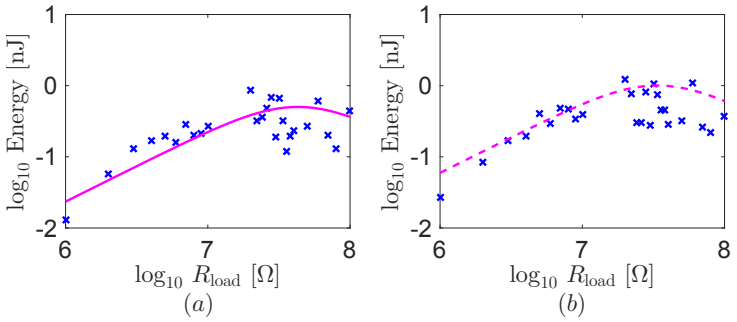

Figure 11. Theoretical predictions and experimental results on energy transferred to the load resistance as a function of the resistance using the human index finger. (**a**) One click and (**b**) double click. Blue crosses and purple lines are the experimental results and the theoretical predictions, respectively.

5. Conclusions

In this paper, we have analyzed energy harvesting from mouse click motions using a piezoelectric material. We have developed a mathematical model for the electromechanical behavior of the system to predict the energy harvested from the finger motion during the mouse clicks. The finger motion has been described as a three degree of freedom mechanism consisting of three links in a plane. The electromechanical coupling of the piezoelectric material has been considered a relationship between its stored charge and rotation angle. To validate the modeling framework, we have conducted experiments about harvested energy at the varying load resistances. As the test subject, we have used a robot finger and a human index finger. The energy harvester has been attached to the both fingers by using a glove with a pocket.

Theoretical predictions of energy harvesting have been found to be in good agreement with experimental results for the both human and robot fingers, corroborating the validity of the proposed modeling approach. Our results indicate that energy harvesting is optimized when the load resistance matches the impedance of the piezoelectric material for the fundamental harmonic, and the maximum harvested energy is in the range of 1–10 nJ. We anticipate that the energy level can be improved by using multiple layers or alternative smart materials with high efficiency. We expect that the experimental results and the modeling framework presented in this study can find application in the design of self-powered mouse or wearable devices through energy harvesting from human motions.

Acknowledgments: This material is based upon work supported by the Global Frontier R & D Program on "Human-centered Interaction for Coexistence" funded by the National Research Foundation of Korea grant funded by the Korean Government (MSIP) (2011-0031425).

Author Contributions: Youngsu Cha led the experiment and modeling, performed data analysis, and drafted the manuscript. Jin Hong conducted the experiment. Jung-Min Park contributed to the setup of the experiment. Jaemin Lee and Keehoon Kim contributed to the operation and the setup of the robot finger.

Conflicts of Interest: The authors declare no conflict of interest.

References

1. Stoppa, M.; Chiolerio, A. Wearable electronics and smart textiles: A critical review. *Sensors* **2014**, *14*, 11957–11992.
2. Zeng, W.; Shu, L.; Li, Q.; Chen, S.; Wang, F.; Tao, X.M. Fiber-based wearable electronics: A review of materials, fabrication, devices, and applications. *Adv. Mater.* **2014**, *26*, 5310–5336.
3. Bahk, J.H.; Fang, H.; Yazawa, K.; Shakouri, A. Flexible thermoelectric materials and device optimization for wearable energy harvesting. *J. Mater. Chem. C* **2015**, *3*, 10362–10374.
4. Kim, M.K.; Kim, M.S.; Lee, S.; Kim, C.; Kim, Y.J. Wearable thermoelectric generator for harvesting human body heat energy. *Smart Mater. Struct.* **2014**, *23*, 105002.
5. Kymissis, J.; Kendall, C.; Paradiso, J.; Gershenfeld, N. Parasitic power harvesting in shoes. In Proceedings of the 2nd IEEE International Symposium on Wearable Computers, Pittsburgh, PA, USA, 19–20 October 1998; pp. 132–139.
6. Renaud, M.; Fiorini, P.; van Schaijk, R.; van Hoof, C. Harvesting energy from the motion of human limbs: The design and analysis of an impact-based piezoelectric generator. *Smart Mater. Struct.* **2009**, *18*, 035001.
7. Delnavaz, A.; Voix, J. Flexible piezoelectric energy harvesting from jaw movements. *Smart Mater. Struct.* **2014**, *23*, 105020.
8. Sodano, H.A.; Inman, D.J.; Park, G. Comparison of piezoelectric energy harvesting devices for recharging batteries. *J. Intell. Mater. Syst. Struct.* **2005**, *16*, 799–807.
9. Erturk, A.; Inman, D.J. *Piezoelectric Energy Harvesting*; John Wiley & Sons, Inc.: Chichester, West Sussex, UK, 2011.
10. Elvin, N.; Erturk, A. (Eds.) *Advances in Energy Harvesting Methods*; Springer-Verlag: London, UK, 2013.
11. Erturk, A.; Inman, D.J. An experimentally validated bimorph cantilever model for piezoelectric energy harvesting from base excitations. *Smart Mater. Struct.* **2009**, *18*, 025009.
12. Shahab, S.; Gray, M.; Erturk, A. Ultrasonic power transfer from a spherical acoustic wave source to a free-free piezoelectric receiver: Modeling and experiment. *J. Appl. Phys.* **2015**, *117*, 104903.
13. Panciroli, R.; Porfiri, M. Hydroelastic impact of piezoelectric structures. *Int. J. Impact Eng.* **2014**, *66*, 18–27.
14. Vatansever, D.; Hadimani, R.L.; Shah, T.; Siores, E. An investigation of energy harvesting from renewable sources with PVDF and PZT. *Smart Mater. Struct.* **2011**, *20*, 055019.
15. Jiang, Y.; Shiono, S.; Hamada, H.; Fujita, T.; Higuchi, K.; Maenaka, K. Low-frequency energy harvesting using a laminated PVDF cantilever with a magnetic mass. *Power MEMS* **2010**, *2010*, 375378.
16. Akaydin, H.D.; Elvin, N.; Andreopoulos, Y. Energy harvesting from highly unsteady fluid flows using piezoelectric materials. *J. Intell. Mater. Syst. Struct.* **2010**, *21*, 1263–1278.
17. Zizys, D.; Gaidys, R.; Dauksevicius, R.; Ostasevicius, V.; Daniulaitis, V. Segmentation of a vibro-shock cantilever-type piezoelectric energy harvester operating in higher transverse vibration modes. *Sensors* **2015**, *15*, doi:10.3390/s16010011.

18. Yang, Y.; Tang, L.; Li, H. Vibration energy harvesting using macro-fiber composites. *Smart Mater. Struct.* **2009**, *18*, 115025.
19. Erturk, A.; Delporte, G. Underwater thrust and power generation using flexible piezoelectric composites: An experimental investigation toward self-powered swimmer-sensor platforms. *Smart Mater. Struct.* **2011**, *20*, 125013.
20. Cha, Y.; Kim, H.; Porfiri, M. Energy harvesting from underwater base excitation of a piezoelectric composite beam. *Smart Mater. Struct.* **2013**, *22*, 115026.
21. Cha, Y.; Chae, W.; Kim, H.; Walcott, H.; Peterson, S.D.; Porfiri, M. Energy harvesting from a piezoelectric biomimetic fish tail. *Renew. Energy* **2016**, *86*, 449–458.
22. Jackson, N.; Keeney, L.; Mathewson, A. Flexible-CMOS and biocompatible piezoelectric AlN material for MEMS applications. *Smart Mater. Struct.* **2013**, *22*, 115033.
23. Gao, P.X.; Song, J.; Liu, J.; Wang, Z.L. Nanowire piezoelectric nanogenerators on plastic substrates as flexible power sources for nanodevices. *Adv. Mater.* **2007**, *19*, 67–72.
24. Shen, D. *Piezoelectric Energy Harvesting Devices for Low Frequency Vibration Applications*; ProQuest: Ann Arbor, MI, USA, 2009.
25. Kim, H.S.; Kim, J.H.; Kim, J. A review of piezoelectric energy harvesting based on vibration. *Int. J. Precis. Eng. Manuf.* **2011**, *12*, 1129–1141.
26. Peng, M. Wireless Mouse Capable of Generating and Accumulating Electrical Energy. US Patent 6686903, 3 February 2004.
27. Bajramovic, M.B. Computer Mouse on a Glove. US Patent 7057604 , 6 June 2006.
28. Kessler, G. D.; Hodges, L.F.; Walker, N. Evaluation of the CyberGlove as a whole-hand input device. *ACM Trans. Comput. Hum. Interact.* **1995**, *2*, 263–283.
29. Granstrom, J.; Feenstra, J.; Sodano, H.A.; Farinholt, K. Energy harvesting from a backpack instrumented with piezoelectric shoulder straps. *Smart Mater. Struct.* **2007**, *16*, 1810.
30. Pozzi, M.; Zhu, M. Plucked piezoelectric bimorphs for knee-joint energy harvesting: Modelling and experimental validation. *Smart Mater. Struct.* **2011**, *20*, 055007.
31. Proto, A.; Penhaker, M.; Bibbo, D.; Vala, D.; Conforto, S.; Schmid, M. Measurements of generated energy/electrical quantities from locomotion activities using piezoelectric wearable sensors for body motion energy harvesting. *Sensors* **2016**, *16*, doi:10.3390/s16040524.
32. De Pasquale, G.; Kim, S.G.; De Pasquale, D. GoldFinger: Wireless human-machine interface with dedicated software and biomechanical energy harvesting system. *IEEE/ASME Trans. Mechatron.* **2016**, *21*, 565–575.
33. Saravanakumar, B.; Mohan, R.; Thiyagarajan, K.; Kim, S.J. Fabrication of a ZnO nanogenerator for eco-friendly biomechanical energy harvesting. *RSC Adv.* **2013**, *3*, 16646–16656.
34. Turner, M.L. Programming Dexterous Manipulation by Demonstration. Ph.D. Thesis, Stanford University, Stanford, CA, USA, 2001.
35. Rohling, R.N.; Hollerbach, J.M. Modeling and parameter estimation of the human index finger. In Proceedings of the IEEE International Conference on Robotics and Automation, San Diego, CA, USA, 8–13 May 1994; pp. 223–230.
36. Maurini, C.; Porfiri, M.; Pouget, J. Numerical methods for modal analysis of stepped piezoelectric beams. *J. Sound Vib.* **2006**, *298*, 918–933.
37. Kim, K. Robot Finger Structure. Korea Patent 1016107450000, 4 April 2016.
38. Lee, J.; Hwang, D.; Kim, M.; Kim, K. A Feasibility Test of Underactuated Prosthetic Robotic Fingers Actuated by Shape Memory Alloy. In Proceedings of the IEEE RAS & EMBS International Conference on Biomedical Robotics and Biomechatronics, Singapore, 26–29 June 2016.